Continuous-wave photoacoustic microscopy

Konstantin Maslov, Lihong V. Wang

Konstantin Maslov, Lihong V. Wang, "Continuous-wave photoacoustic microscopy," Proc. SPIE 6437, Photons Plus Ultrasound: Imaging and Sensing 2007: The Eighth Conference on Biomedical Thermoacoustics, Optoacoustics, and Acousto-optics, 64370P (13 February 2007); doi: 10.1117/12.702240

SPIE.

Event: SPIE BiOS, 2007, San Jose, California, United States

Continuous-wave photoacoustic microscopy

Konstantin Maslov and Lihong V. Wang*
Optical Imaging Laboratory, Department of Biomedical Engineering, Washington University in St. Louis, MO 63123-1097

ABSTRACT

We have built a photoacoustic microscope (PAM) using an amplitude-modulated continuous-wave (CW) laser source, which is an inexpensive 120-mW laser diode. By using a bowl-shaped piezoelectric transducer, whose numerical aperture is 0.85 and resonance frequency is 2.45 MHz, we have experimentally demonstrated a lateral resolution of 600 μm, an axial resolution of 700 μm, and a signal-to-noise ratio (SNR) as high as 43 dB. Although the SNR in the CW PAM system is an order of magnitude worse than that of the pulsed-laser-based PAM system, CW PAM shows potential for biomedical applications as it uses durable and inexpensive semiconductor lasers, which will significantly reduce operation costs of the PAM systems.

Keywords: medical and biological imaging, photoacoustic imaging, microscopy

1. INTRODUCTION

Reflection-mode photoacoustic microscopy with a pulsed laser and a high numerical aperture ultrasonic transducer has shown the ability to image microvascular networks in the skin.[1-8] The current photoacoustic microscopy using pulsed laser illumination is capable of imaging with ~15 μm axial resolution and 45-120 μm lateral resolution. The signal to noise ratio for large rat vessels is ~40 dB[9]. Photoacoustic imaging reveals physiologically specific optical absorption contrast. PA imaging takes advantage of the weaker ultrasonic scattering, whose magnitude is two orders of magnitude less than that of optical scattering[10] to achieve high spatial resolution in deep biological tissues compared with traditional optical imaging[11,12]. In addition, PA imaging is able to extract certain functional parameters, such as the hemoglobin oxygenation saturation (SO_2), without using exogenous contrast agents by varying the optical wavelength of the excitation laser and conducting spectroscopic measurement.

In state-of-the-art laser PA instrumentation and measurement techniques pulsed lasers have always been the PA signal source of choice. The major reasons for this choice are a large amount of the available energy in a laser pulse thus yielding acceptable signal-to-noise ratios (SNR) under transient pulse detection[13], and possibility to localize optically absorbing volume by measuring time of flight of ultrasonic transient generated by short optical pulse. That increase SNR, simplifies interpretation of PA signal and diminish complex interference effects caused by coherent photoacoustic radiation.

Pulsed PA detection, however, presents disadvantages in terms of laser jitter noise and acoustic and thermal noise within the wide bandwidth of the transducer, In addition, very large pulsed-laser peak irradiances incident on living tissue may have detrimental effects, and for this reason very low average pulse energies are used at the expense of SNR.

Frequency-domain PA methodologies can offer alternative detection and imaging schemes with several advantages over pulsed laser photoacoustics. These advantages include a low fluence of the harmonic or frequency-swept modulated laser light with the concomitant advantage of lower possibility of tissue damage. The superior signal-to-noise ratio of the ultra-narrow lock-in amplifier bandpass filter can offset much of the SNR deterioration at MHz frequencies. Frequency chirps may also be used to recover the axial resolution. The chirp can be further tailored to center around a particular depth of interest, thus offering an efficient rejection of undesirable acoustic signals outside the time window minimizing unwanted interference effects.

Photons Plus Ultrasound: Imaging and Sensing 2007: The Eighth Conference on Biomedical Thermoacoustics, Optoacoustics, and Acousto-optics, edited by Alexander A. Oraevsky, Lihong V. Wang,
Proc. of SPIE Vol. 6437, 64370P, (2007) · 1605-7422/07/$18 · doi: 10.1117/12.702240

Simplification of quantitative measurements is an additional advantage of the CW PAM. For example, instrumental normalization procedure can be done through a simple division with a reference signal in the frequency-domain, as opposed to nontrivial deconvolution in the time domain, especially with highly nonlinear resonant ultrasonic transducers.

And last but not least advantage is low equipment and operational costs of the CW modulated lasers. Inconvenience and expense of photoacoustic technique which mostly comes from reliance on high energy short duration light pulses available only from laboratory grade tunable Q-switch pumped lasers is one of the major obstacles for its wide application in medicine and biology. In contrast CW modulated semiconductor lasers are durable, does not require highly qualified personal to operate, and significantly safer for patient and operator in case of accidental exposure.

The CW photoacoustic microscopy with lock-in detection system has already displayed feasibility to measure surface[14] as well as subsurface[15] properties in solids. In this study we investigated possibility to obtain photoacoustic image using convenient lased diode as a source of optical illumination.

Although at megahertz frequencies photoacoustic tomography (PAT)[1-5] is typically used for CW photoacoustic imaging detection useful tool is photoacoustic microscopy[16]. In PAT, an inverse reconstruction algorithm based on time of flight of acoustic transient is employed to acquire image of biological samples which gives very poor resolution for band-limited CW photoacoustic imaging. In contrast, scanning photoacoustic microscopy (PAM) having spatial resolution defined by properties of the spherically-focused ultrasonic detector is well suited for CW photoacoustic imaging.

In this article we will report physical realization of CW PAM and compare developed CW PAM to state of the art table-top dark-field illumination PAM[9,16] .

2. METHODOLOGY

Because laser diodes have relatively peak power, which is several orders less than Q-switch lasers, special attention should be paid to of signal to noise ratio of the CW PAM. To compare it to that of PAM with pulse excitation at maximum permissible radiation exposure let us consider peak acoustic pressure generated by localized light absorption. Regardless of absorber geometry[17,18,19] PA pressure far from absorber, p, is proportional to $\kappa \cdot \dot{Q}$, where $\kappa = \beta \cdot c^2 \dot{Q} / C_p$, β is thermal expansion coefficient, c is speed of sound, C_p is heat capacity per unit mass and $\dot{Q}$ is time derivative of heat deposition per unit volume. For pulse excitation, time dependence of heat deposition can be approximated by Gaussian function $Q \approx \mu_a E_p \exp\left(\omega_p^2 t^2\right)$, where μ_a is light absorption coefficient I_p is peak optical intensity, $1/\omega_p$ is the pulse width and ω_p is cut-off frequency of the PA transient. After simple algebraic manipulations maximum PA pressure can be related to peak intensity as: $p_{p,\max} \propto \sqrt{\frac{2}{e}} \omega_p I_p$. Similarly stationary heat deposition in case of CW PAM is defined by $Q \approx \mu_a I_{CW} \left(1 + \sin\left(\omega_c t\right)\right)$, where ω_c is modulation frequency. Corresponding acoustic pressure is given by $p_{CW,\max} \propto \omega_c I_{CW}$. Let us assume that condition for equal spatial resolution of the CW and pulse PAM is $\omega_p = \omega_c$. For a signal to noise ratio (SNR) estimate it is good enough approximation. For both CW PAM and pulse PAM maximum peak intensity of the laser light is limited by safety concern governed by ANSI safety standard[20], which limits maximum permissible pulse exposure to 20mJ/cm^2 of pulse energy per unit area of human skin and CW exposure to 200mW/cm^2. Simple calculations shows that safety limited peak acoustic pressure for 100ns pulse excitation can be six orders higher than acoustic pressure amplitude of CW PAM. However, broad-band nature of pressure transient suggests much higher noise amplitude of pulse PAM which is proportional to square root of the bandwidth of PA signal. For pulse PAM bandwidth is related to cut-off frequency $\Delta f_p \propto \omega_p / 2\pi$ for CW PAM it can be as narrow as image sampling frequency which for table-top PAM under comparison is equal to 10Hz. Final estimate gives for CW PAM with sub-millimeter resolution signal to noise ratio must be about three orders worse than that of pulse PAM. Taken into account that at best SNR of PAM is between 40dB and 60dB[Error! Bookmark not defined.] it seemed that pressure waves generated by CW PAM are undetectable.

However, SNR of the CW PAM can be significantly improved. Firstly, broad-band piezoelectric transducers have high insertion loss, which typically of the order of 20dB[21], due to low electromechanical coupling of polymer piezoelectric and strong mismatch of acoustic impedance if piezo-ceramic. Piezoelectric transducer for CW application does not have to be acoustically matched to immersion liquid because near its through-thickness resonance input impedance of the transducer changes from very low to very high and there always be a frequency at which it is equal to impedance of the immersion liquid. Because resonant CW transducer also does not have resonance damping backing material its insertion loss is limited to electrical loss due to finite conductivity of piezoelectric and mechanical losses in piezoceramic. Together at a few megahertz frequency these losses can be as little as a few dB.

Another possibility to improve SNR of the CW PAM is in using low duty cycle tone bursts amplitude modulation instead of CW modulation. According to ANSI standard for less than 10s exposure the maximum permissible exposure is limited by $1100t_e^{1/4}$ in mJ/cm2, where t_e denotes the exposure duration in seconds. For 10 Hz pulse repetition frequency with 1% duty cycle it gives maximum permissible exposure of 20W/cm^2 thus improving SNR on one order of magnitude. Altogether these made CW PAM at least feasible for some biomedical applications.

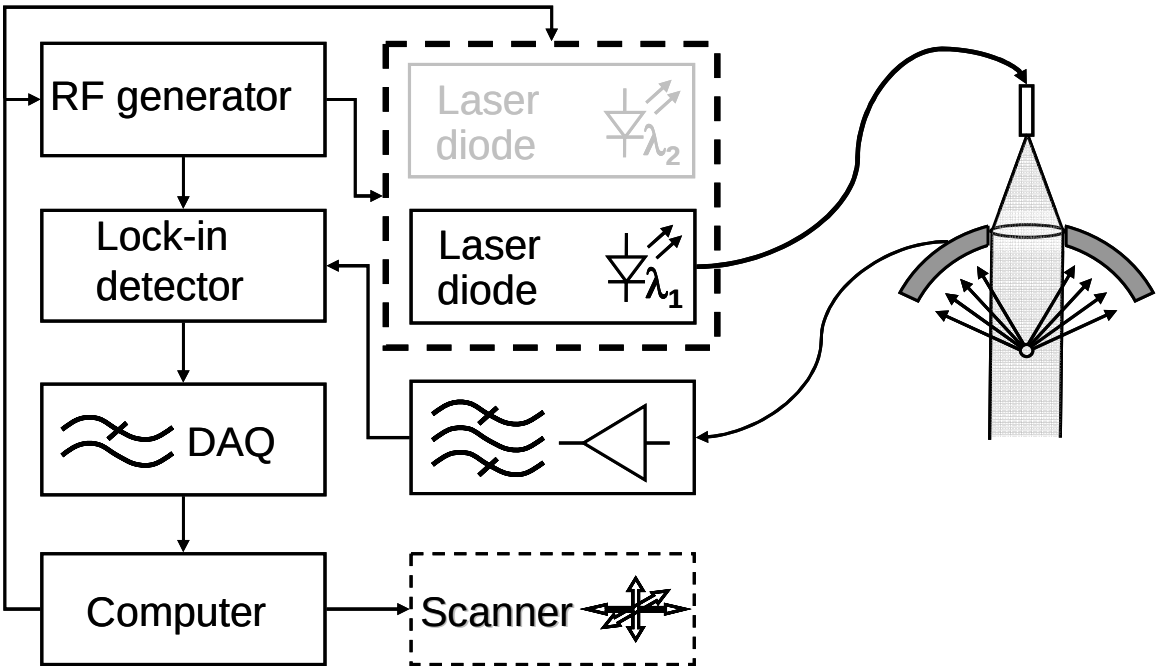

Fig.1. Schematic of the CW PAM.

To verify feasibility of CW PAM we built simple PAM system shown in Fig. 1. We have used inexpensive laser diode (Sharp, GH0781JA2C 120W 784nm) driven by LDC220 laser diode current controller (Thorlabs Inc.). We use100% amplitude modulation of the laser diode at 2.45 MHz by applying 10V sinusoidal signal from function generator through serial 50Ohm resistor. PA signal from resonant piezo-transducer was amplified by narrow-band preamplifier and detected by lack-in amplifier (SR844, Stanford Research Systems) which was used as phase sensitive detector and data acquisition system. Amplitude and phase of the transducer signal was analyzed by personal computer which also control mechanical scanner used for raster scanning of the sample.

Light from laser diode was delivered to transducer via single fiber. It is passing through collimating lens secured within the hole on axis of bowl shaped piezoceramic element as shown in fig.2 and delivered to the sample surface. Piezo-ceramic element of the transducer has hemi-spherical shape of 38mm diameter and 11mm radius of curvature with gold electrodes on both sides of the sphere. Outer electrode seen in Fig.2 was soldered to the transducer shell with low melting point alloy (SnCuInCd eutectic). Inner electrode is connected to resonant preamplifier via impedance matching line transformer.

Fig.2. Photo of the resonant photoacoustic transducer.

All experimental human procedures were carried out in conformity with the guidelines of the US National Institutes of Health. The laboratory animal and human protocols for this work were approved by the University Laboratory Animal Care Committee of Texas A&M University.

3. RESULTS

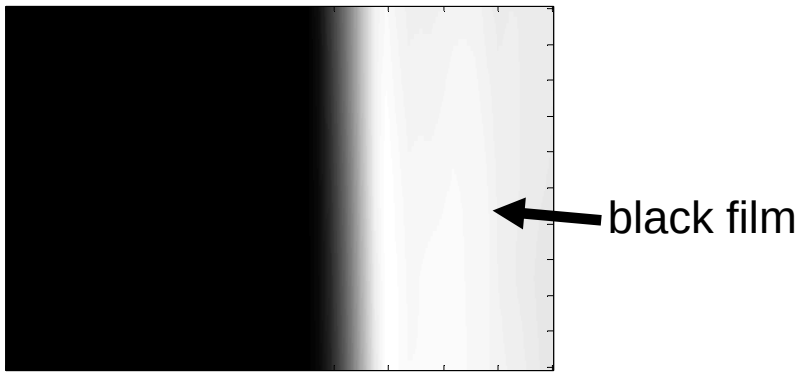

Fig.3. CW PAM Image of the edge of black polyethylene film.

An estimate of SNR has been made by imaging the edge of highly optically absorptive black polyethylene film. Image contrast in Fig.3 is 43 dB. It must be no less than system SNR which gives for CW PAM in clear media SNR better than 43 dB. Lateral resolution of the CW PAM has been tested by using USAF 1951 test target. The modulation transfer function[22], was extracted from the peak-to peak signal and extrapolated to the cut-off spatial frequency. Estimated lateral resolution of 600 μm was found to be good agreement with theoretical value for 0.85 NA spherical transducer.

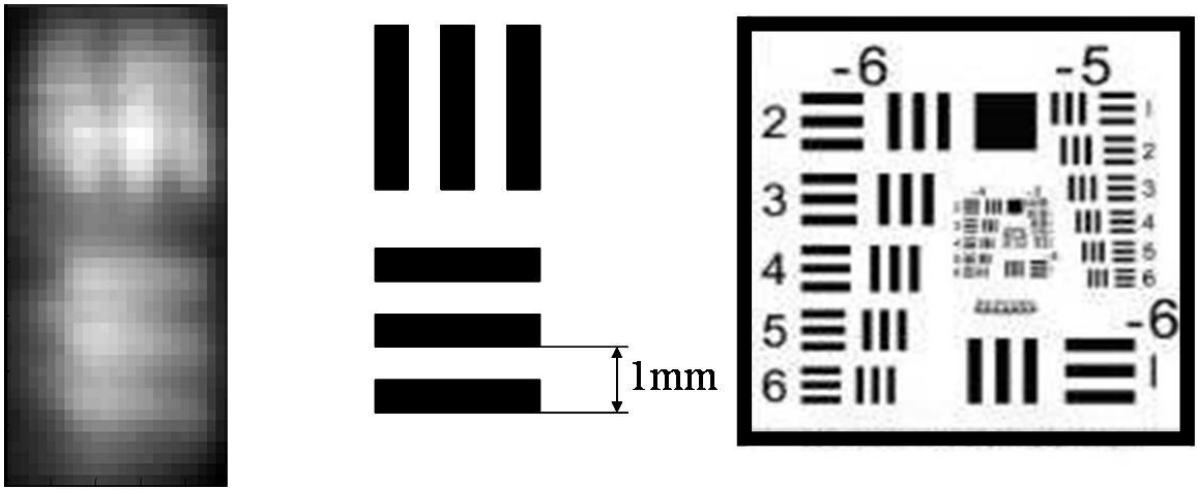

Fig.4. Resolution test of the CW PAM using USAF 1951 test target.

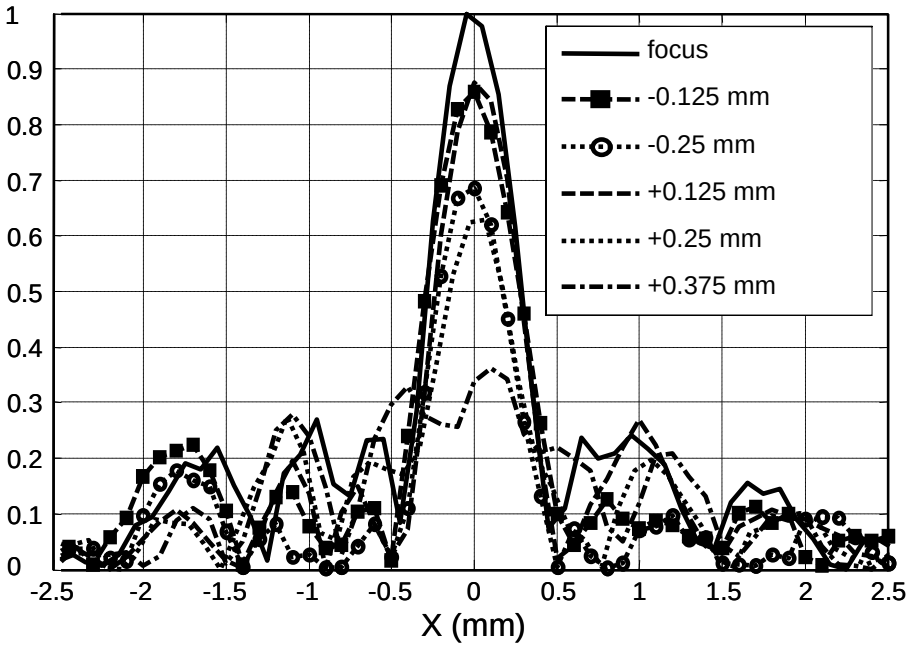

Fig. 5. Line spread function of the CW PAM transducer.

Axial (and lateral) resolution has been measured by scanning thin light absorptive cylinder (human hair) immersed in light scattering media (0.2% imtralipid). Line spread functions axial positions of the fiber with respect of the focal plane of the PAM are shown in Fig5. Estimated -6dB axial resolution was about 0.7 mm which is close to expected value for such a high NA spherically focused transducer.

In situ CW PAM amplitude image of the rabbit ear vasculature is shown in Fig.6A. Raster scanning was performed with scanning speed 10 steps (image pixels) per second, lock-in integration time was 30ms. One can see that CW PAM has enough resolution and sensitivity to show major blood vessels. However, in some places image is difficult to interpret. Reason for that is in presence of multiple acoustic arrivals which can interfere with each other. In addition, there is the possibility of complex interference effects on the sample surface due to ultrasonic reflections from sample boundaries and/or surface of the transducer. Direct penetration of the modulation signal into lack-in input is also possible.

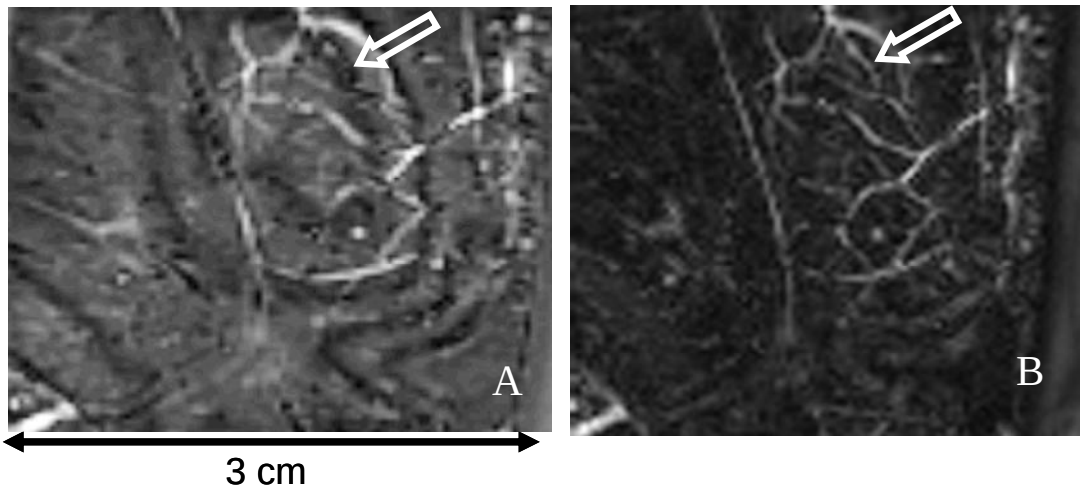

Fig.6. *In situ* CW PAM image of vasculature of rabbit ear.

To rectify interference problem PA wave source localization can be performed by sweeping modulation frequency within frequency band of the transducer[14.] Source localization idea is based on a simple property of the Fourier transform. In frequency domain, transducer voltage is proportional to the PA wave pressure, $p(\omega)$ multiplied on frequency response on the ultrasonic receiver which also includes ultrasonic attenuation in the media and phase shift due to PA wave propagation from its origin to ultrasonic transducer. In time-space domain it become a convolution of PA wave source axial location, $p(z)$, where $z = ct$ with Fourier transform of the transducer response. That can be illustrated by a simple example. Let us suppose that frequency response of the resonant transducer has Gaussian shape and phase shift is caused by wave propagating distance z_0 to the transducer:

$$V(\omega) \propto p(\omega) \cdot \exp\left(-(\omega - \omega_0)^2 / \Delta\omega^2\right) \cdot \exp\left(i\omega z_0 / c\right). \tag{1}$$

In space domain we have:

$$V(z) \propto p(z) \otimes \exp - \left(\pi \frac{(z - z_0)}{\Lambda} \frac{\Delta\omega}{\omega_0} \right)^2, \tag{2}$$

where Λ is wavelength of PA wave at frequency ω_0. One can see that localization of the PA source is about ultrasonic wavelength multiplied on a factor of $\omega_0 / \pi\Delta\omega$. In real case frequency response must be experimentally measured during setup calibration by recording amplitude and phase of the signal from the test target placed in focal spot of the transducer as a function of modulation frequency and continuous Fourier transform can be replaced by discrete Fourier transform. Moreover, in many cases use of a very few frequencies is enough to remove some most significant image artifacts.

An application of the above described procedure is illustrated in Fig.7. Fig.7B shows B-scan image of the blood vessel at 1 mm depth in rat skin taken by pulse PAM[16] equipped with 5 MHz transducer. Fig.7B shows sweep frequency reconstructed B-scan image taken by the same PAM but with CW excitation at frequencies ranging from 4.5MHz to 5.5MHz with 40KHz step. Taken into account that for resonant transducer $\Delta\omega << \omega_0$ frequency sweep cannot substitute B-scan image yet can be successfully used to remove interference artifacts as it illustrated in Fig.6B. Here we supposed that interference of PA signal from blood vessels and from front surface of the transducer occur. Hence we have used only two frequencies shifted by $\Delta f = c / 2z_0$ and simply subtract one PA signal from another. As it can bee seen in Fig.6 that was enough to significantly improve image quality and simplify image interpretation. Some blood vessels which show inverted contrast along their length in Fig6A, for example one indicated by arrow, looks uniformly bright in Fig6B.

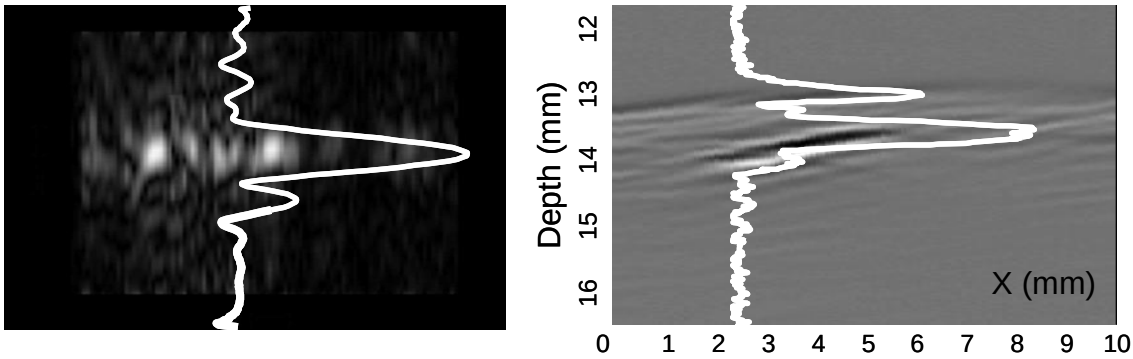

Fig.7. Blood vessel at 1 mm depth in rat skin, A-B-scan taken by pulse PAM equipped with 5MHz ultrasonic transducer. B- sweep frequency reconstructed B-scan image taken by CW PAM.

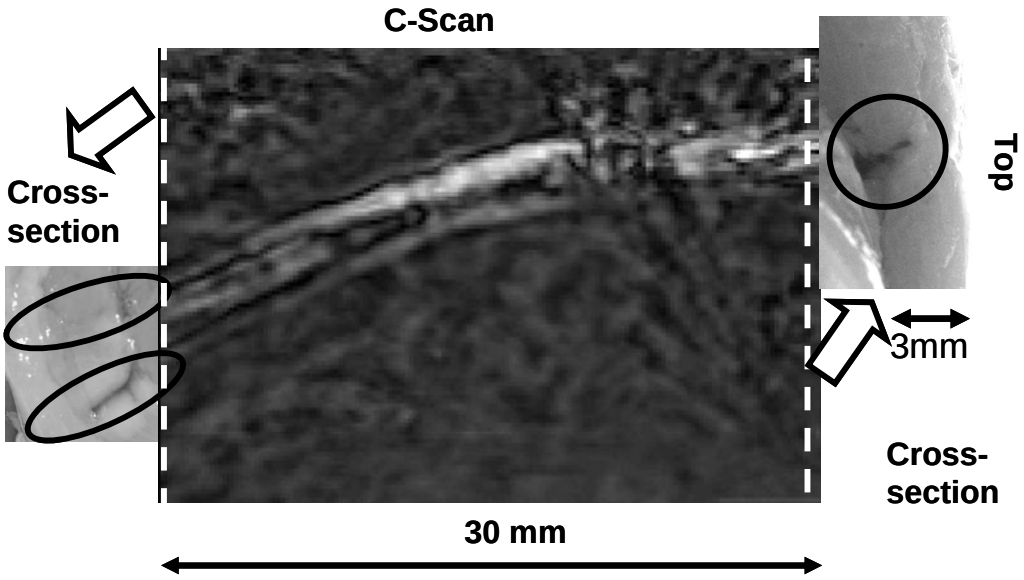

Fig.8. *In situ* CW PAM image of the rabbit tibial blood vessels

Ability CW PAM to image subsurface structures has been verified by *In situ* CW PAM imaging of the blood vessels in rabbit leg as shown in Fig8. Bright colored structure shown in figure is tibial artery and vein located about 3mm below skin surface as revealed by anatomical sectioning also shown in Fig.8.

4. CONCLUSION AND DISCUSSION

Feasibility of using continuous wave modulated light source in photoacoustic imaging for biomedical application has been tested. Although, experimentally achieved SNR was an order worse than that of pulse PAM, CW PAM shows some potential for biomedical application because it uses durable and inexpensive semiconductor laser which does not require highly qualified personal and are safer for both patient and operator in case of accidental exposure. Small depth of focus does not allow CW PAM to compete with pulse, Q-switch laser based PAM in imaging speed, but with the use of several laser diodes having laser emission of wavelengths of choice covering wide range of wavelengths CW PAM can be very competitively used for noninvasive localized quantitative spectral absorption measurements *in vivo*.

5. ACKNOWLEDGEMENTS

This project is sponsored by National Institutes of Health grants R01 EB000712 and R01 NS46214.

6. REFERENCES

1. Xu, M. & Wang, L. V. Photoacoustic imaging in biomedicine. *Rev. Sci. Instrum.* 77, 041101 (2006).
2. Wang, X. *et. al.* Noninvasive laser-induced photoacoustic tomography for structural and functional imaging of the brain in vivo. *Nature Biotechnol.* 21, 803–806 (2003).
3. Hoelen, C.G.A., de Mul, F.F.M., Pongers, R. & Dekker, A. Three-dimensional photoacoustic imaging of blood vessels in tissue. *Opt. Lett.* 23, 648–650 (1998).
4. Oraevsky, A.A. & Karabutov, A.A. Optoacoustic Tomography. in *Biomedical Photonics Handbook*, Vol. PM125 (ed. Vo-Dinh, T.) CRC Press, Boca Raton, Florida, 2003.
5. Kruger, R.A., Liu, P., Fang, Y.R. & Appledorn, C.R. Photoacoustic ultrasound (PAUS) – reconstruction tomography. *Med. Phys.* 22, 1605–1609 (1995).
6. Bell, A.G. On the production and reproduction of sound by light. *Am. J. Sci*. 20, 305–324 (1880).
7. Diebold, G.J., Khan, M.I. & Park, S.M. Photoacoustic "signature" of particulate matter: optical production of acoustic monopole radiation. *Science* 250, 101–104 (1990).
8. Tam, A.C. Applications of photoacoustic sensing techniques, *Rev. Mod. Phys.* 58, 381–431 (1986).
9. Zhang, H.F., Maslov, K., Stoica, G & Wang, L.V. Functional photoacoustic microscopy for high-resolution and noninvasive *in vivo* imaging. *Nat. Biotechnol*. 24, 848–851 (2006).
10. Duck, F. A. *Physical Properties of Tissue,* (Academy Press London, 1990.
11. Oleary, M.A., Boas, D.A., Chance, B. & Yodh, A.G. Experimental images of heterogeneous turbid media by frequency-domain diffuse-photon tomography. *Opt. Lett.* 20, 426–428 (1995).
12. Boas, D.A., Brooks, D.H., Miller, E.L., DiMarzio, C.A., Kilmer, M., Gaudette, R.J. & Zhang, Q. Imaging the body with diffuse optical tomography. *IEEE Signal Processing Magazine* 18, 57–75 (2001).
13. A. Oraevsky and A. Karabutov, ''Ultimate sensitivity of time-resolved opto-acoustic detection,'' *Biomedical Optoacoustics*, Proc. SPIE Vol. 3916, 228–239 A. A. Oraevsky, Ed., Bellingham, WA, 2000.
14. T. W. Murray and O. Balogun, "High-sensitivity laser-based acoustic microscopy using a modulated excitation source"Applied Physics Letters 85, 2974, (2004).
15. Ying Fan, A. Mandelis, G. Spirou and I. A. Vitkin "Development of a laser photothermoacoustic frequency-swept system for subsurface imaging: Theory and experiment" J. Acoust. Soc. Am. 116 3523-3533 (2004).
16. Maslov, K., Stoica, G. & Wang, L.V. *In vivo* dark-field reflection-mode photoacoustic microscopy. *Opt. Lett.* 30, 625–627 (2005).
17. M.I. Khan and G.J. Diebold "The photoacoustic effect generated by an isotropic solid sphere" Ultrasonics 33 265-269 (1995).
18. M.I. Khan, G.J. Diebold "The photoacoustic effect generated by laser irradiation of an isotropic solid cylinder" Ultrasonics 34 19-24 (1996).
19. G. J. Diebold, T. Sun, and M. I. Khan, "Photoacoustic Monopole Radiation in One, Two, and Three Dimensions," Physical Review Letters, 69 (9), 3384-3387, (1991).
20. Laser Institute of America, *American National Standard for Safe Use of Lasers ANSI Z136.1-2000,* American National Standards Institute, Inc., New York, NY, 2000.
21. M. Robert, G. Molingou, and K. Snook "Fabrication of focused poly.vinylidene fluoride-trifluoroethylene PVDF-TrFE copolymer 40–50 MHz ultrasound transducers on curved surfaces" *Journal Of Applied Physics* 96 252-257 (2004).
22. W. J. Smith, "Modern Optical Engineering," McGrew-Hill, New York, 1966, p. 318.

*lhwang@biomed.wustl.edu; phone 1 314 935-6152; fax 1 314 935-7448